Cite as: M. D. Kornberg *et al.*, *Science* 10.1126/science.aan4665 (2018).

Dimethyl fumarate targets GAPDH and aerobic glycolysis to modulate immunity

Michael D. Kornberg,[1] Pavan Bhargava,[1] Paul M. Kim,[2] Vasanta Putluri,[3] Adele M. Snowman,[4] Nagireddy Putluri,[3,5] Peter A. Calabresi,[1,4] Solomon H. Snyder[2,4,6]*

[1]Department of Neurology, Johns Hopkins University School of Medicine, Baltimore, MD 21287, USA. [2]Department of Psychiatry and Behavioral Sciences, Johns Hopkins University School of Medicine, Baltimore, MD 21287, USA. [3]Advanced Technology Core, Baylor College of Medicine, Houston, TX 77030, USA. [4]Department of Neuroscience, Johns Hopkins University School of Medicine, Baltimore, MD 21205, USA. [5]Department of Molecular and Cellular Biology, Baylor College of Medicine, Houston, TX 77030, USA. [6]Department of Pharmacology and Molecular Sciences, Johns Hopkins University School of Medicine, Baltimore, MD 21205, USA.

*Corresponding author. Email: ssnyder@jhmi.edu

Activated immune cells undergo a metabolic switch to aerobic glycolysis akin to the Warburg effect, presenting a potential therapeutic target in autoimmune disease. Dimethyl fumarate, a derivative of the Krebs cycle intermediate fumarate, is an immunomodulatory drug used to treat multiple sclerosis and psoriasis. Although its therapeutic mechanism remains uncertain, it covalently modifies cysteine residues in a process termed "succination." Here, we show that dimethyl fumarate succinates and inactivates the catalytic cysteine of the glycolytic enzyme GAPDH both in vitro and in vivo. It thereby downregulates aerobic glycolysis in activated myeloid and lymphoid cells, which mediates its anti-inflammatory effects. Our findings provide mechanistic insight into immune modulation by dimethyl fumarate and represent a proof of concept that aerobic glycolysis is a therapeutic target in autoimmunity.

Pro-inflammatory stimuli induce a metabolic switch in both myeloid and lymphoid cells, leading to a Warburg-like upregulation of aerobic glycolysis that regulates the balance between inflammatory and regulatory immune phenotypes (*1*, *2*). Classically activated macrophages and effector lymphocytes such as T-helper (Th) 1 and Th17 cells require glycolysis for their survival, differentiation, and effector functions (*3*–*9*), whereas oxidative metabolism favors the differentiation of alternatively activated (M2) macrophages and regulatory T (Treg) cells (*10*, *11*).

Dimethyl fumarate (DMF) is a serendipitously discovered immunomodulatory drug used to treat psoriasis and multiple sclerosis (MS) (*12*). Although its mechanisms of action remain incompletely understood, it is known to covalently modify cysteine residues in a process termed "succination" (not to be confused with lysine succinylation) (fig. S1) (*13*, *14*). DMF succinates kelch-like ECH-associated protein 1 (KEAP1), which activates nuclear factor (erythroid-derived 2)-related factor 2 (Nrf2) to produce anti-oxidant and anti-inflammatory effects that nonetheless fail to fully account for the drug's actions (*15*). Endogenous fumarate also succinates proteins, with a primary target being the active-site cysteine of the glycolytic enzyme glyceraldehyde 3-phosphate dehydrogenase (GAPDH) (*16*). In this study, we show that DMF and its clinically relevant metabolite monomethyl fumarate (MMF) target GAPDH and inactivate its enzyme activity, both in vitro and after oral treatment in mice and humans. In turn, GAPDH inhibition downregulates aerobic glycolysis in myeloid and lymphoid cells, preventing immune activation and shifting the balance between inflammatory and regulatory cell types.

To determine whether GAPDH was succinated by DMF and MMF, we performed liquid chromatography–tandem mass spectrometry (LC–MS/MS). Treatment of recombinant human GAPDH with MMF led to monomethyl succination (2-monomethyl succinyl-cysteine) at its active-site cysteine (Cys-152 in human) and cysteines 156 and 247, whereas DMF produced a combination of dimethyl (2-dimethyl succinyl-cysteine) and monomethyl succination at the same cysteines (table S1 and fig. S2). Neither of these modifications was observed at any cysteine in vehicle-treated GAPDH. In mice, oral treatment with DMF led to both monomethyl and dimethyl succination exclusively of the active-site cysteine (Cys-150 in mouse) of GAPDH purified from the spleen and brain, with no such modifications observed on other cysteines or in vehicle-treated mice (Fig. 1A and table S1). Although only the monomethyl form of the drug is detected in serum (*17*), our finding that dimethyl succination occurred after oral administration was consistent with prior work (*18*, *19*). Monomethyl succination of GAPDH Cys-152 was also identified in peripheral blood mononuclear cells (PBMCs) from MS patients treated with DMF (Fig. 1B and table S1) but not on other cysteines or in PBMCs from MS patients not treated with DMF. GAPDH succination by endogenous fumarate occurred physiologically, as we identified modification by fumarate (2-succinyl-

cysteine) at the active-site cysteine in vehicle-treated mice and human healthy controls (fig. S3).

Covalent modification of its catalytic cysteine should irreversibly inactivate GAPDH. We found that both DMF and MMF decreased the catalytic activity of recombinant GAPDH in a dose- and time-dependent manner (Fig. 1C). This inhibition was irreversible, as desalting failed to restore activity (fig. S4A). Additionally, this inhibition was mediated by active-site binding of DMF/MMF, as the drug effect was blocked by pre-incubation with tenfold excess of GAPDH substrates (fig. S4B). GAPDH inhibition was biphasic, with an initial fast phase and a secondary slow phase. We calculated the kinetics of inhibition for both phases using the Kitz–Wilson method (*20*) (fig. S4C). GAPDH activity was similarly inhibited in cultured mouse peritoneal macrophages (mPMs) treated overnight with 25 μM DMF (Fig. 1D). In mice, oral treatment with DMF decreased GAPDH activity measured from both the spleen and small intestine (Fig. 1E). This effect was particularly profound in the small intestine, which may be relevant given the role of the gut immune system in autoimmune disorders such as MS (*21*).

We next asked whether GAPDH inhibition by DMF impacted aerobic glycolysis in activated immune cells. Using lactate production as a proxy measure, co-treatment with DMF significantly impaired glycolysis in mPMs stimulated in vitro for 24 hours with 1 μg/ml lipopolysaccharide (LPS) (Fig. 2A). MMF had a similar effect but with lower potency. The influence on glycolysis was not due to cytotoxicity (fig. S5). Measurements of the extracellular acidification rate (ECAR) revealed a similar inhibition of aerobic glycolysis by DMF and MMF in LPS-stimulated mPMs (Fig. 2B). In activated mouse and human $CD4^+$ lymphocytes, DMF and MMF decreased basal glycolysis, with an even greater effect on maximal glycolytic capacity (Fig. 2C and fig. S6). In LPS-stimulated mPMs, treatment with DMF produced a blockade in glycolytic flux at GAPDH (Fig. 2D and fig. S7), providing evidence that GAPDH inactivation mediated the downregulation of glycolysis by DMF.

DMF had no effect on glycolysis in unstimulated mPMs (Fig. 2E), raising the possibility that DMF acts not only on GAPDH but also on the signaling pathway required for glycolytic upregulation. However, DMF had no effect on the activity of mechanistic target of rapamycin (mTOR, as measured via p70-S6 kinase phosphorylation) or levels of hypoxia-inducible factor 1-α (HIF-1α) (Fig. 2F and fig. S8). This selective inhibition of glycolysis in LPS-stimulated mPMs is consistent with recent evidence that GAPDH only becomes a rate-limiting enzyme when glycolysis is upregulated in the setting of Warburg physiology (*22–24*), as it is in cancer and activated immune cells. This likely explains why DMF is not generally toxic.

We also examined whether DMF impacted oxidative phosphorylation (OXPHOS). DMF increased OXPHOS in mPMs under both resting and LPS-stimulated conditions (fig. S9A). The inhibition of glycolysis did not depend on the upregulation of OXPHOS (fig. S9, B and C).

We next asked whether inhibition of GAPDH and aerobic glycolysis mediated the immunologic actions of DMF. We first addressed this question in macrophages. We reproduced previous findings that both DMF and glycolytic blockade prevent classical macrophage activation (fig. S10, A to D) (*3*, *25*) and then determined that the inhibition of cytokine production by DMF was unrelated to its effects on OXPHOS (fig. S10E). We next measured the production of IL-1β under low (0.5 mM) or high (10 mM) glucose concentrations and found that DMF was much less effective in the presence of high glucose (Fig. 3A), suggesting that its anti-inflammatory effect can be overcome by driving glycolysis higher with saturating concentrations of glucose. DMF augmented the IL-4-induced expression of arginase-1 (Arg-1), a marker of M2 alternative activation (fig. S10F), but the relative importance of DMF effects on aerobic glycolysis versus OXPHOS in promoting alternative activation was not examined.

Heptelidic acid (also known as koningic acid) is a GAPDH inhibitor, which binds the active site and covalently modifies the catalytic cysteine (*23*, *26*). The treatment of mPMs with heptelidic acid replicated the effects of DMF on IL-1β secretion (Fig. 3B), inducible nitric oxide synthase (iNOS) expression (Fig. 3C and fig. S11A), and nuclear translocation of nuclear factor-κB (NF- κB) (Fig. 3D and fig. S11B). Conversely, the overexpression of wild-type GAPDH, but not catalytically inactive GAPDH mutated at Cys-150, mitigated the effect of DMF on IL-1β production (Fig. 3E and fig. S12). Thus, the immunologic actions of DMF were replicated by GAPDH inhibition and reversed by increasing GAPDH expression.

We next examined the effects of DMF and MMF on lymphocyte differentiation and function. We activated mouse naïve $CD4^+$ T cells under Th1-, Th17-, or Treg-cell-polarizing conditions for four days ± DMF or MMF, with treatment at the start of polarization. Consistent with known effects of glycolytic blockade (*7*, *8*), DMF disproportionately impacted the survival of Th1 and Th17 versus Treg cells (Fig. 4A and fig. S13A). Similarly, DMF/MMF inhibited both differentiation and cytokine production under Th1- and Th17-polarizing conditions, an effect replicated by heptelidic acid (Fig. 4, B to D, and fig. S13B). As reported with HIF-1α deficiency and 2-deoxyglucose (*11*), DMF promoted Treg-cell differentiation under Treg-polarizing conditions (Fig. 4E and fig. S13B), and both DMF and MMF reciprocally inhibited Th17 and promoted Treg cell development under Th17-polarizing conditions (Fig. 4F). When added after three days of polarization, DMF, MMF, and low-dose heptelidic

acid had no effect on viability (fig. S14A) or differentiation (fig. S14B) of Th1 or Th17 cells. However, all three drugs inhibited the expression of IFNγ and IL-17 (Fig. 4G), suggesting an effect on cytokine production independent of survival and differentiation.

Because GAPDH binding to mRNA underlies post-transcriptional regulation of cytokine production (*9*), we tested the effect of GAPDH succination on RNA binding (fig. S15). Pre-treatment with DMF (or heptelidic acid) decreased GAPDH–RNA binding, as reported with other modifications of the active-site cysteine (*27*). This effect was small, however, as a similar decrease was produced by a tenfold lower concentration of NAD^+. Thus, the alteration of such binding does not appear to underlie the immunologic actions of DMF.

Finally, to ascertain whether GAPDH inhibition produced anti-inflammatory actions in vivo, we examined the effect of heptelidic acid in experimental autoimmune encephalomyelitis (EAE), a mouse model of MS, and found that it attenuated the disease in these mice (Fig. 4H).

By demonstrating that a known immunomodulatory drug acts by inhibiting aerobic glycolysis, our findings provide a proof of concept that metabolism is a viable therapeutic target in autoimmunity. They may also explain important observations of DMF therapy in patients. DMF differentially impacts distinct lymphocyte subsets, producing lymphopenia that selectively depletes highly glycolytic effector T cells while sparing oxidative naïve T cells and Treg cells (*28*, *29*). Our findings suggest that the inhibition of aerobic glycolysis underlies these selective effects. It is also notable that DMF is simply a derivative of fumarate, which is a metabolic intermediate of the Krebs cycle, lying downstream of glycolysis in cellular energy production. We hypothesize that fumarate-induced inactivation of GAPDH represents an endogenous negative feedback loop. DMF—a more cell-permeable and electrophilic derivative of fumarate—may simply exploit this physiologic pathway to produce its immunologic actions (Fig. 4I). It must be noted, however, that additional targets of succination (in addition to KEAP1) are likely relevant to both the therapeutic and toxic effects of the drug.

REFERENCES AND NOTES

1. E. L. Pearce, E. J. Pearce, Metabolic pathways in immune cell activation and quiescence. *Immunity* **38**, 633–643 (2013). doi:10.1016/j.immuni.2013.04.005 Medline

2. B. Kelly, L. A. O'Neill, Metabolic reprogramming in macrophages and dendritic cells in innate immunity. *Cell Res.* **25**, 771–784 (2015). doi:10.1038/cr.2015.68 Medline

3. G. M. Tannahill, A. M. Curtis, J. Adamik, E. M. Palsson-McDermott, A. F. McGettrick, G. Goel, C. Frezza, N. J. Bernard, B. Kelly, N. H. Foley, L. Zheng, A. Gardet, Z. Tong, S. S. Jany, S. C. Corr, M. Haneklaus, B. E. Caffrey, K. Pierce, S. Walmsley, F. C. Beasley, E. Cummins, V. Nizet, M. Whyte, C. T. Taylor, H. Lin, S. L. Masters, E. Gottlieb, V. P. Kelly, C. Clish, P. E. Auron, R. J. Xavier, L. A. J. O'Neill, Succinate is an inflammatory signal that induces IL-1β through HIF-1α. *Nature* **496**, 238–242 (2013). doi:10.1038/nature11986 Medline

4. C. M. Cham, T. F. Gajewski, Glucose availability regulates IFN-γ production and p70S6 kinase activation in $CD8^+$ effector T cells. *J. Immunol.* **174**, 4670–4677 (2005). doi:10.4049/jimmunol.174.8.4670 Medline

5. C. M. Cham, G. Driessens, J. P. O'Keefe, T. F. Gajewski, Glucose deprivation inhibits multiple key gene expression events and effector functions in $CD8^+$ T cells. *Eur. J. Immunol.* **38**, 2438–2450 (2008). doi:10.1002/eji.200838289 Medline

6. R. Wang, C. P. Dillon, L. Z. Shi, S. Milasta, R. Carter, D. Finkelstein, L. L. McCormick, P. Fitzgerald, H. Chi, J. Munger, D. R. Green, The transcription factor Myc controls metabolic reprogramming upon T lymphocyte activation. *Immunity* **35**, 871–882 (2011). doi:10.1016/j.immuni.2011.09.021 Medline

7. A. N. Macintyre, V. A. Gerriets, A. G. Nichols, R. D. Michalek, M. C. Rudolph, D. Deoliveira, S. M. Anderson, E. D. Abel, B. J. Chen, L. P. Hale, J. C. Rathmell, The glucose transporter Glut1 is selectively essential for CD4 T cell activation and effector function. *Cell Metab.* **20**, 61–72 (2014). doi:10.1016/j.cmet.2014.05.004 Medline

8. V. A. Gerriets, R. J. Kishton, A. G. Nichols, A. N. Macintyre, M. Inoue, O. Ilkayeva, P. S. Winter, X. Liu, B. Priyadharshini, M. E. Slawinska, L. Haeberli, C. Huck, L. A. Turka, K. C. Wood, L. P. Hale, P. A. Smith, M. A. Schneider, N. J. MacIver, J. W. Locasale, C. B. Newgard, M. L. Shinohara, J. C. Rathmell, Metabolic programming and PDHK1 control $CD4^+$ T cell subsets and inflammation. *J. Clin. Invest.* **125**, 194–207 (2015). doi:10.1172/JCI76012 Medline

9. C. H. Chang, J. D. Curtis, L. B. Maggi Jr., B. Faubert, A. V. Villarino, D. O'Sullivan, S. C.-C. Huang, G. J. W. van der Windt, J. Blagih, J. Qiu, J. D. Weber, E. J. Pearce, R. G. Jones, E. L. Pearce, Posttranscriptional control of T cell effector function by aerobic glycolysis. *Cell* **153**, 1239–1251 (2013). doi:10.1016/j.cell.2013.05.016 Medline

10. D. Vats, L. Mukundan, J. I. Odegaard, L. Zhang, K. L. Smith, C. R. Morel, R. A. Wagner, D. R. Greaves, P. J. Murray, A. Chawla, Oxidative metabolism and PGC-1β attenuate macrophage-mediated inflammation. *Cell Metab.* **4**, 13–24 (2006). doi:10.1016/j.cmet.2006.05.011 Medline

11. L. Z. Shi, R. Wang, G. Huang, P. Vogel, G. Neale, D. R. Green, H. Chi, HIF1α-dependent glycolytic pathway orchestrates a metabolic checkpoint for the differentiation of T_H17 and T_{reg} cells. *J. Exp. Med.* **208**, 1367–1376 (2011). doi:10.1084/jem.20110278 Medline

12. R. A. Linker, A. Haghikia, Dimethyl fumarate in multiple sclerosis: Latest developments, evidence and place in therapy. *Ther. Adv. Chronic Dis.* **7**, 198–207 (2016). doi:10.1177/2040622316653307 Medline

13. R. A. Linker, D.-H. Lee, S. Ryan, A. M. van Dam, R. Conrad, P. Bista, W. Zeng, X. Hronowsky, A. Buko, S. Chollate, G. Ellrichmann, W. Brück, K. Dawson, S. Goelz, S. Wiese, R. H. Scannevin, M. Lukashev, R. Gold, Fumaric acid esters exert neuroprotective effects in neuroinflammation via activation of the Nrf2 antioxidant pathway. *Brain* **134**, 678–692 (2011). doi:10.1093/brain/awq386 Medline

14. M. M. Blewett, J. Xie, B. W. Zaro, K. M. Backus, A. Altman, J. R. Teijaro, B. F. Cravatt, Chemical proteomic map of dimethyl fumarate-sensitive cysteines in primary human T cells. *Sci. Signal.* **9**, rs10 (2016). doi:10.1126/scisignal.aaf7694 Medline

15. U. Schulze-Topphoff, M. Varrin-Doyer, K. Pekarek, C. M. Spencer, A. Shetty, S. A. Sagan, B. A. C. Cree, R. A. Sobel, B. T. Wipke, L. Steinman, R. H. Scannevin, S. S. Zamvil, Dimethyl fumarate treatment induces adaptive and innate immune modulation independent of Nrf2. *Proc. Natl. Acad. Sci. U.S.A.* **113**, 4777–4782 (2016). doi:10.1073/pnas.1603907113 Medline

16. M. Blatnik, N. Frizzell, S. R. Thorpe, J. W. Baynes, Inactivation of glyceraldehyde-3-phosphate dehydrogenase by fumarate in diabetes: Formation of S-(2-succinyl)cysteine, a novel chemical modification of protein and possible biomarker of mitochondrial stress. *Diabetes* **57**, 41–49 (2008). doi:10.2337/db07-0838 Medline

17. N. H. Litjens, J. Burggraaf, E. van Strijen, C. van Gulpen, H. Mattie, R. C. Schoemaker, J. T. van Dissel, H. B. Thio, P. H. Nibbering, Pharmacokinetics of oral fumarates in healthy subjects. *Br. J. Clin. Pharmacol.* **58**, 429–432 (2004). doi:10.1111/j.1365-2125.2004.02145.x Medline

18. M. Rostami-Yazdi, B. Clement, T. J. Schmidt, D. Schinor, U. Mrowietz, Detection of metabolites of fumaric acid esters in human urine: Implications for their mode of action. *J. Invest. Dermatol.* **129**, 231–234 (2009). doi:10.1038/jid.2008.197 Medline

19. H. Peng, H. Li, A. Sheehy, P. Cullen, N. Allaire, R. H. Scannevin, Dimethyl fumarate alters microglia phenotype and protects neurons against proinflammatory toxic microenvironments. *J. Neuroimmunol.* **299**, 35–44 (2016). doi:10.1016/j.jneuroim.2016.08.006 Medline

20. Z. D. Parsons, K. S. Gates, Redox regulation of protein tyrosine phosphatases: Methods for kinetic analysis of covalent enzyme inactivation. *Methods Enzymol.* **528**, 129–154 (2013). doi:10.1016/B978-0-12-405881-1.00008-2

21. N. Kamada, S. U. Seo, G. Y. Chen, G. Núñez, Role of the gut microbiota in immunity and inflammatory disease. *Nat. Rev. Immunol.* **13**, 321–335 (2013). doi:10.1038/nri3430 Medline

22. A. A. Shestov, X. Liu, Z. Ser, A. A. Cluntun, Y. P. Hung, L. Huang, D. Kim, A. Le, G. Yellen, J. G. Albeck, J. W. Locasale, Quantitative determinants of aerobic glycolysis identify flux through the enzyme GAPDH as a limiting step. *eLife* **3**, 03342 (2014). Medline

23. M. V. Liberti, Z. Dai, S. E. Wardell, J. A. Baccile, X. Liu, X. Gao, R. Baldi, M. Mehrmohamadi, M. O. Johnson, N. S. Madhukar, A. A. Shestov, I. I. C. Chio, O. Elemento, J. C. Rathmell, F. C. Schroeder, D. P. McDonnell, J. W. Locasale, A predictive model for selective targeting of the Warburg effect through GAPDH inhibition with a natural product. *Cell Metab.* **26**, 648–659.e8 (2017). doi:10.1016/j.cmet.2017.08.017 Medline

24. J. Yun, E. Mullarky, C. Lu, K. N. Bosch, A. Kavalier, K. Rivera, J. Roper, I. I. C. Chio, E. G. Giannopoulou, C. Rago, A. Muley, J. M. Asara, J. Paik, O. Elemento, Z. Chen, D. J. Pappin, L. E. Dow, N. Papadopoulos, S. S. Gross, L. C. Cantley, Vitamin C selectively kills KRAS and BRAF mutant colorectal cancer cells by targeting GAPDH. *Science* **350**, 1391–1396 (2015). doi:10.1126/science.aaa5004 Medline

25. M. A. Michell-Robinson, C. S. Moore, L. M. Healy, L. A. Osso, N. Zorko, V. Grouza, H. Touil, L. Poliquin-Lasnier, A.-M. Trudelle, P. S. Giacomini, A. Bar-Or, J. P. Antel, Effects of fumarates on circulating and CNS myeloid cells in multiple sclerosis. *Ann. Clin. Transl. Neurol.* **3**, 27–41 (2015). doi:10.1002/acn3.270 Medline

26. K. Sakai, K. Hasumi, A. Endo, Identification of koningic acid (heptelidic acid)-modified site in rabbit muscle glyceraldehyde-3-phosphate dehydrogenase. *Biochim. Biophys. Acta* **1077**, 192–196 (1991). doi:10.1016/0167-4838(91)90058-8 Medline

27. E. Nagy, W. F. Rigby, Glyceraldehyde-3-phosphate dehydrogenase selectively binds AU-rich RNA in the NAD^+-binding region (Rossmann fold). *J. Biol. Chem.* **270**, 2755–2763 (1995). doi:10.1074/jbc.270.6.2755 Medline

28. C. M. Spencer, E. C. Crabtree-Hartman, K. Lehmann-Horn, B. A. Cree, S. S. Zamvil, Reduction of $CD8^+$ T lymphocytes in multiple sclerosis patients treated with dimethyl fumarate. *Neurol. Neuroimmunol. Neuroinflamm.* **2**, e76 (2015). doi:10.1212/NXI.0000000000000076 Medline

29. C. C. Gross, A. Schulte-Mecklenbeck, S. Klinsing, A. Posevitz-Fejfár, H. Wiendl, L. Klotz, Dimethyl fumarate treatment alters circulating T helper cell subsets in multiple sclerosis. *Neurol. Neuroimmunol. Neuroinflamm.* **3**, e183 (2015). doi:10.1212/NXI.0000000000000183 Medline

30. M. R. Hara, N. Agrawal, S. F. Kim, M. B. Cascio, M. Fujimuro, Y. Ozeki, M. Takahashi, J. H. Cheah, S. K. Tankou, L. D. Hester, C. D. Ferris, S. D. Hayward, S. H. Snyder, A. Sawa, S-nitrosylated GAPDH initiates apoptotic cell death by nuclear translocation following Siah1 binding. *Nat. Cell Biol.* **7**, 665–674 (2005). doi:10.1038/ncb1268 Medline

31. P. A. Calabresi, R. Allie, K. M. Mullen, S. H. Yun, R. W. Georgantas 3rd, K. A. Whartenby, Kinetics of CCR7 expression differ between primary activation and effector memory states of T_H1 and T_H2 cells. *J. Neuroimmunol.* **139**, 58–65 (2003). doi:10.1016/S0165-5728(03)00127-9 Medline

32. A. Shevchenko, O. N. Jensen, A. V. Podtelejnikov, F. Sagliocco, M. Wilm, O. Vorm, P. Mortensen, A. Shevchenko, H. Boucherie, M. Mann, Linking genome and proteome by mass spectrometry: Large-scale identification of yeast proteins from two dimensional gels. *Proc. Natl. Acad. Sci. U.S.A.* **93**, 14440–14445 (1996). doi:10.1073/pnas.93.25.14440 Medline

33. A. Keller, A. I. Nesvizhskii, E. Kolker, R. Aebersold, Empirical statistical model to estimate the accuracy of peptide identifications made by MS/MS and database search. *Anal. Chem.* **74**, 5383–5392 (2002). doi:10.1021/ac025747h Medline

34. A. I. Nesvizhskii, A. Keller, E. Kolker, R. Aebersold, A statistical model for identifying proteins by tandem mass spectrometry. *Anal. Chem.* **75**, 4646–4658 (2003). doi:10.1021/ac0341261 Medline

35. G. J. van der Windt, C. H. Chang, E. L. Pearce. Measuring bioenergetics in T cells using a Seahorse extracellular flux analyzer. *Curr. Protoc. Immunol.* **113**, 16B.1-16B.14 (2016).

36. V. Vantaku, S. R. Donepudi, C. R. Ambati, F. Jin, V. Putluri, K. Nguyen, K. Rajapakshe, C. Coarfa, V. L. Battula, Y. Lotan, N. Putluri, Expression of ganglioside GD2, reprogram the lipid metabolism and EMT phenotype in bladder cancer. *Oncotarget* **8**, 95620–95631 (2017). doi:10.18632/oncotarget.21038 Medline

37. F. Jin, J. Thaiparambil, S. R. Donepudi, V. Vantaku, D. W. B. Piyarathna, S. Maity, R. Krishnapuram, V. Putluri, F. Gu, P. Purwaha, S. K. Bhowmik, C. R. Ambati, F.-C. von Rundstedt, F. Roghmann, S. Berg, J. Noldus, K. Rajapakshe, D. Gödde, S. Roth, S. Störkel, S. Degener, G. Michailidis, B. A. Kaipparettu, B. Karanam, M. K. Terris, S. M. Kavuri, S. P. Lerner, F. Kheradmand, C. Coarfa, A. Sreekumar, Y. Lotan, R. El-Zein, N. Putluri, Tobacco-specific carcinogens induce hypermethylation, DNA adducts, and DNA damage in bladder cancer. *Cancer Prev. Res.* **10**, 588–597 (2017). doi:10.1158/1940-6207.CAPR-17-0198 Medline

38. D. W. B. Piyarathna, T. M. Rajendiran, V. Putluri, V. Vantaku, T. Soni, F. C. von Rundstedt, S. R. Donepudi, F. Jin, S. Maity, C. R. Ambati, J. Dong, D. Gödde, S. Roth, S. Störkel, S. Degener, G. Michailidis, S. P. Lerner, S. Pennathur, Y. Lotan, C. Coarfa, A. Sreekumar, N. Putluri, Distinct lipidomic landscapes associated with clinical stages of urothelial cancer of the bladder. *Eur. Urol. Focus* **17**, 30107–30114 (2017). Medline

ACKNOWLEDGMENTS

We thank J. Liu and J. Stivers for insights regarding enzyme kinetics experiments. We are grateful to Z. Zhou, W. Chen, and A. Hoke for providing access to the Seahorse extracellular flux analyzer and support with its use. We thank L. DeVine and R. Cole from the Johns Hopkins Mass Spectrometry Core Facility for their assistance and helpful discussion. We are grateful to B. Wipke and R. Scannevin for insightful discussion and for providing a protocol for preparation of DMF suspension. We thank B. Paul for help with mPM isolation and GAPDH–RNA binding, C. Darius for drawing blood samples, and J. Bo for preparation of PBMCs. **Funding:** Funding for M.D.K. was provided by the NINDS (R25 grant, RFA-NS-12-003), National Multiple Sclerosis Society (NMSS) – American Academy of Neurology (AAN) (Clinician Scientist Development Award, FAN 17107-A-1), and Conrad N. Hilton Foundation (Marilyn Hilton Bridging Award). Funding for P.B. was provided by the AAN (John F. Kurtzke Clinician Scientist Development Award), NMSS (Career Transition Award, TA-1503-03465), and Race to Erase MS (Young Investigator Award). V.P. and N.P. were supported by the CPRIT Core Facility Support Award (RP170005), NCI Cancer Center Support Grant (P30CA125123), and intramural funds from the Dan L. Duncan Cancer

Center (DLDCC). N.P. was also supported by the American Cancer Society (127430-RSG-15-105-01-CNE) and NIH (R01CA220297 and R01CA216426). Funding for P.A.C. was provided by the NINDS (R37NS041435). Funding for S.H.S. was provided by USPHS grant MH18501. **Author contributions:** M.D.K., P.B., P.A.C, and S.H.S. contributed to overall project design. M.D.K., P.B., P.M.K., V.P., N.P., and A.M.S. performed the research. M.D.K., P.B., P.M.K., V.P., and N.P., analyzed the data. M.D.K. and P.B. prepared the figures. M.D.K. and S.H.S. wrote the manuscript. P.B., P.A.C., and N.P. edited the manuscript. **Competing interests:** P.A.C. has received research funding in the past from Biogen, the company that sells DMF (trade name Tecfidera) as a therapy for MS. He received a consulting honorarium from Biogen in 2015 for work related to the compound opicinumab. The other authors declare no competing interests. **Data and materials availability:** Data in this paper are presented and/or tabulated in the main text and supplementary materials.

SUPPLEMENTARY MATERIALS

www.sciencemag.org/cgi/content/full/science.aan4665/DC1
Materials and Methods
Table S1
Figs. S1 to S15
References (*30*–*38*)

27 April 2017; resubmitted 29 January 2018
Accepted 15 March 2018
Published online 29 March 2018
10.1126/science.aan4665

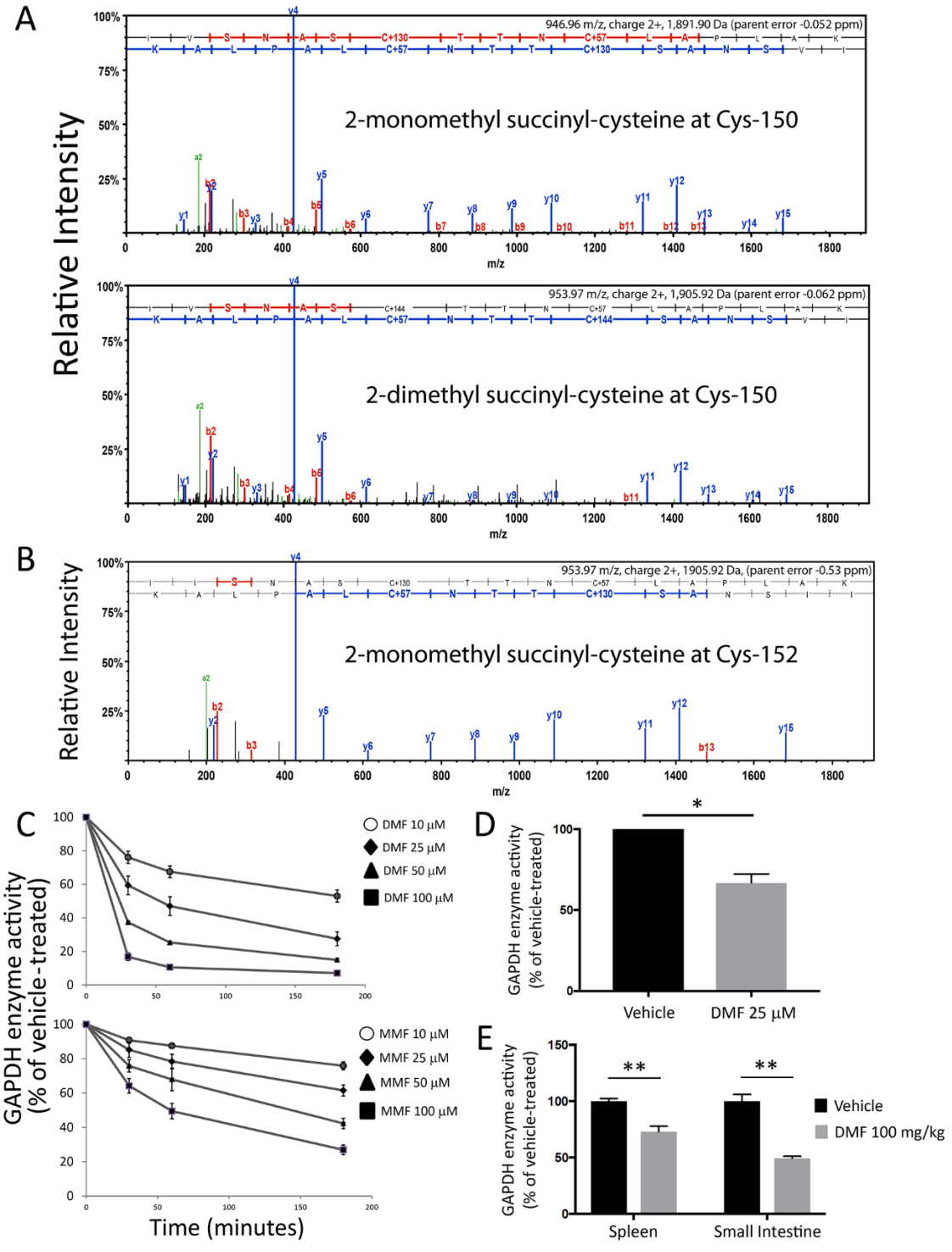

Fig. 1. DMF and MMF succinate and inactivate GAPDH in vitro and after oral treatment. (**A**) Representative LC-MS/MS spectra demonstrating covalent modification of the catalytic cysteine (Cys-150 in mouse) by either monomethyl (2-monomethyl succinyl-cysteine, +130 Da) or dimethyl (2-dimethyl succinyl-cysteine, +144 Da) fumarate in GAPDH immunoprecipitated from splenic lysates of mice treated orally with 100 mg/kg DMF daily for five days. Because samples were reduced and treated with iodoacetate, non-succinated cysteines were modified with carbamidomethyl (Carb, +57 Da). Pooled samples were analyzed from two vehicle-treated and two DMF-treated animals. (**B**) Representative LC-MS/MS spectrum demonstrating monomethyl succination of the catalytic cysteine (Cys-152 in human) of GAPDH immuno-precipitated from PBMC lysates of MS patients treated with DMF for three months. Pooled samples were analyzed from three DMF-treated and two non-DMF-treated patients. (**C**) Dose- and time-dependent inactivation of GAPDH enzyme activity in vitro. Recombinant GAPDH was treated with the indicated drug concentrations or vehicle alone. Aliquots were removed at the specified time points, followed by enzyme activity assay. Data were pooled from four experiments performed in duplicate and represent mean ± SEM for each time point. Associated Kitz–Wilson plots and kinetic parameters are shown in fig. S4C. (**D**) Peritoneal macrophages were treated overnight with DMF. Cells lysates were used for GAPDH enzyme activity assay. Data represent mean ± SEM of three experiments performed in duplicate. (**E**) Mice were treated with DMF 100 mg/kg daily for five days by oral gavage. On Day 5, mice were sacrificed, and lysates from spleen and small intestine were used for GAPDH enzyme activity assay. Data represent mean ± SEM of five mice per group, with assays run in triplicate. Da = daltons. $*P < 0.05$ and $**P < 0.01$ by two-tailed Student's *t*-test.

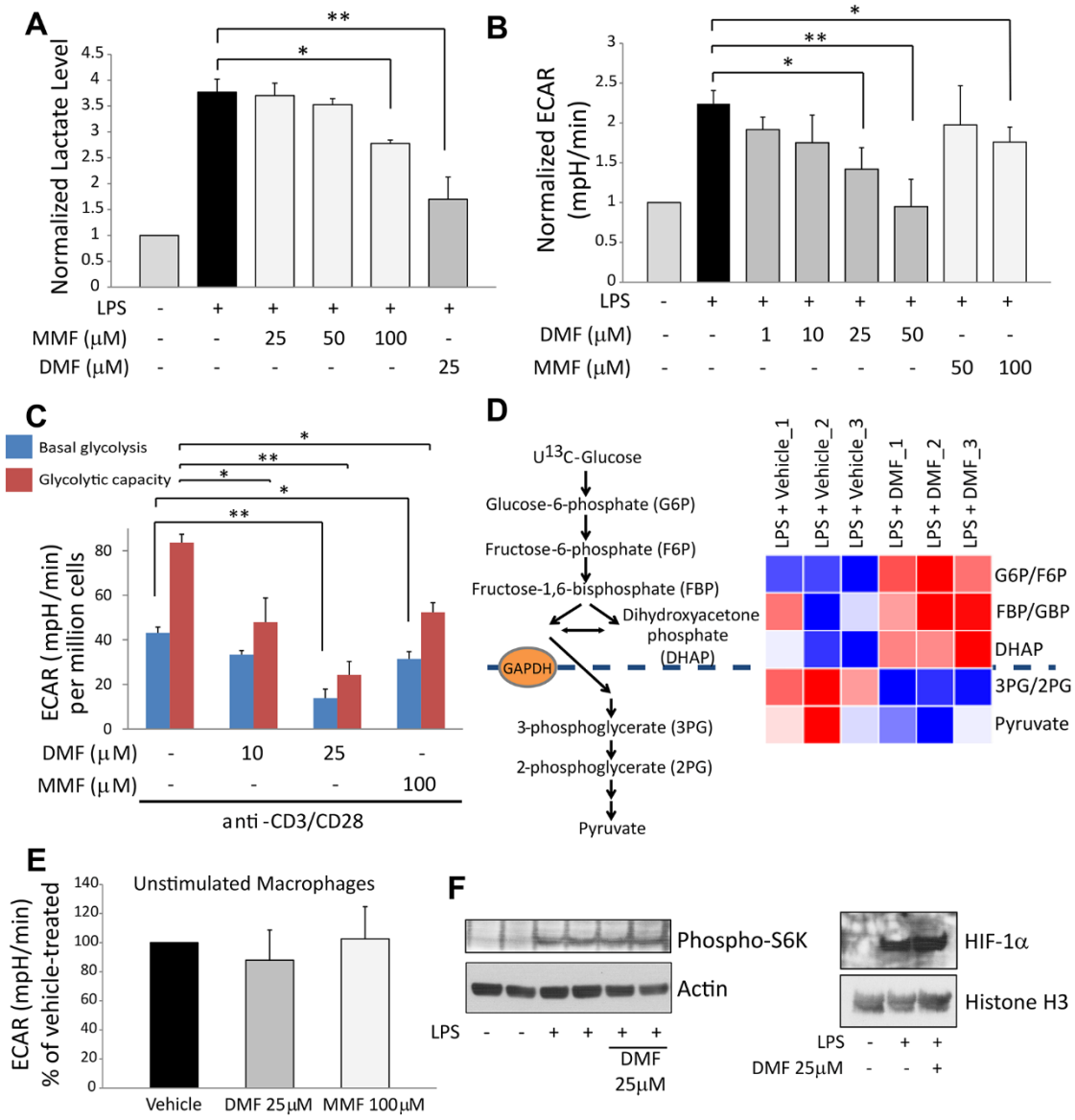

Fig. 2. GAPDH inactivation by DMF and MMF inhibits glycolysis in activated, but not resting, macrophages and lymphocytes. (**A**) Mouse peritoneal macrophages (mPMs) were treated with LPS ± DMF or MMF for 24 hours followed by measurement of lactate (a proxy measure of glycolysis) in culture media by colorimetric assay. Data represent mean ± SEM of three experiments performed in duplicate. (**B**) mPMs were treated as in (A), and glycolysis was measured as extracellular acidification rate (ECAR) using a Seahorse extracellular flux analyzer. Data represent mean ± SEM of five experiments performed in quadruplicate. (**C**) Glycolysis was measured via Seahorse extracellular flux analyzer in mouse naive $CD4^+$ lymphocytes activated overnight with anti-CD3/CD28 antibodies ± DMF/MMF. Data represent mean ± SEM of four experiments performed in triplicate. (**D**) mPMs were stimulated with LPS for 24 hours ± 25 μM DMF, in triplicate. Cells were then labeled with $U^{13}C$-glucose, and ^{13}C-labeling of glycolytic intermediates was measured from lysates via LC-MS. Heat map shows blockade of glycolytic flux at the level of GAPDH. (**E**) DMF/MMF had no effect on glycolysis in unstimulated mPMs, measured as ECAR. Data represent mean ± SEM of four experiments performed in quadruplicate. (**F**) Representative immunoblots showing no effect of DMF on phospho-S6K (a marker of mTOR activity) (*N* = two experiments performed in duplicate) or HIF-1α levels (*N* = three experiments) in LPS-stimulated mPMs. Data are quantified in fig. S8. $*P < 0.05$ and $**P < 0.01$ by one-way analysis of variance (ANOVA) with Dunnett's multiple comparison.

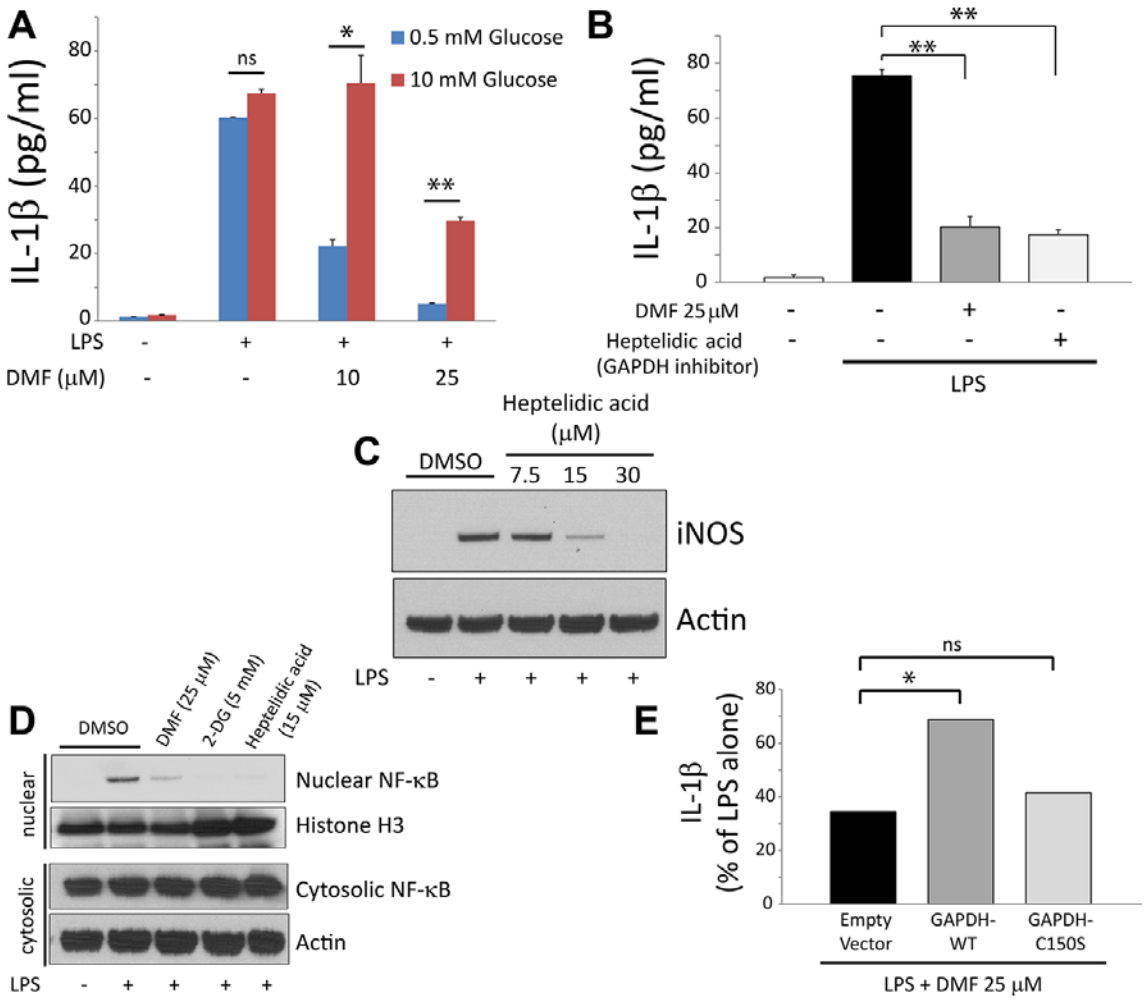

Fig. 3. Inhibition of GAPDH and aerobic glycolysis mediates anti-inflammatory effects of DMF in macrophages. (**A**) mPMs were treated with LPS ± DMF for 24 hours in either limiting (0.5 mM) or saturating (10 mM) concentrations of glucose, followed by measurement of IL-1β secretion by ELISA. Data represent mean ± SEM of three experiments performed in singlet or duplicate. (**B**) Treating LPS-stimulated mPMs with 30 μM heptelidic acid, a selective GAPDH inhibitor, replicated the effect of DMF on IL-1β secretion. Data represent mean ± SEM of three experiments performed in singlet or duplicate. (**C** and **D**) Representative immunoblots from three experiments showing that heptelidic acid replicated the effects of DMF on iNOS expression (C) and nuclear translocation of NF-κB (D) in LPS-stimulated mPMs. Data are quantified in fig. S11. (**E**) Overexpression of wild-type GAPDH (GAPDH-WT), but not Cys-150 mutant (GAPDH-C150S), mitigated the effect of DMF on IL-1β secretion in mPMs. Data represent the mean of two experiments performed in duplicate. ns = non-significant. **P* < 0.05 and ***P* < 0.01 by two-tailed Student's *t*-test (A) and one-way ANOVA with Dunnett's multiple comparison (B and E).

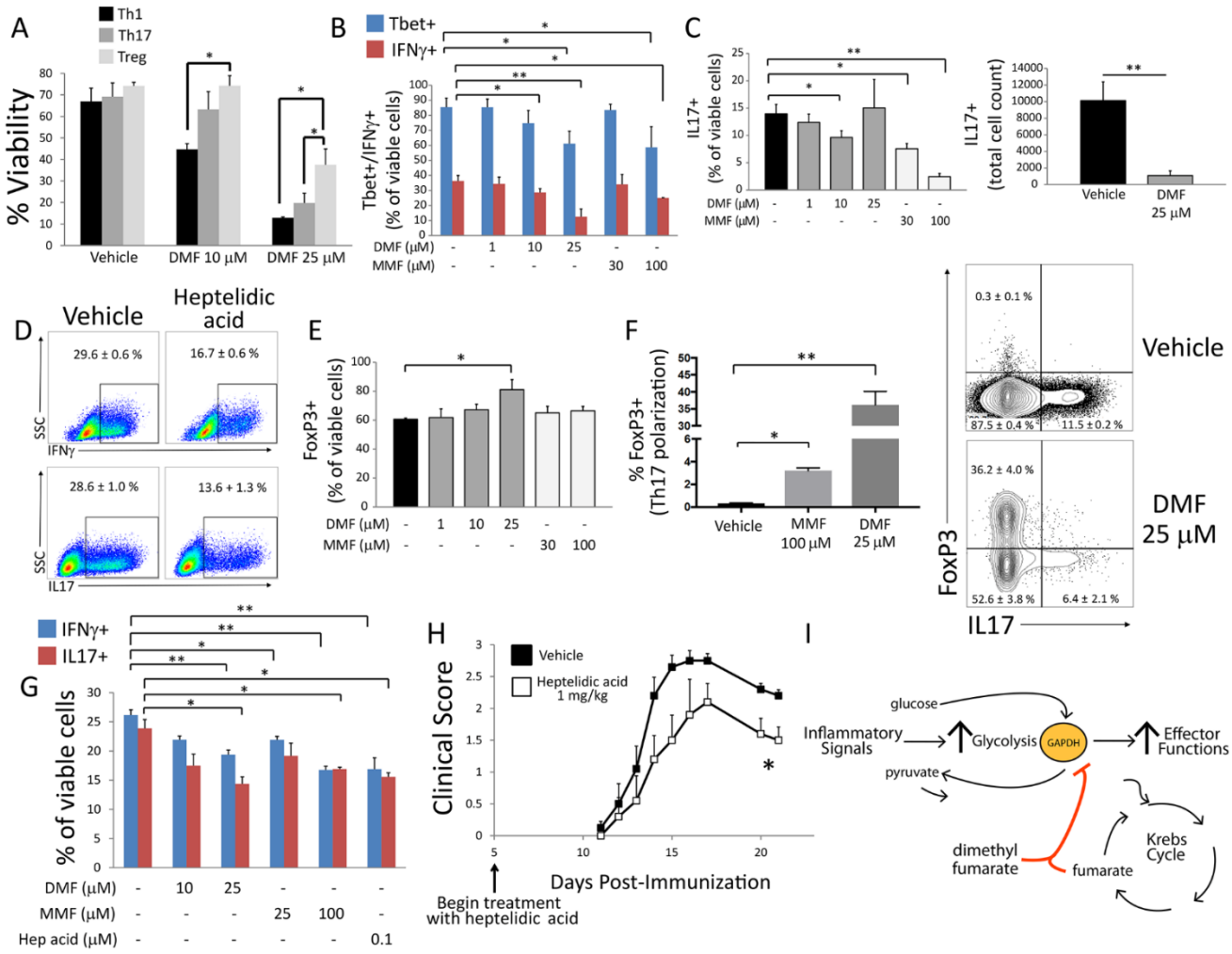

Fig. 4. DMF and MMF differentially impact survival, differentiation, and effector function of metabolically distinct lymphocyte subsets. (**A** to **F**) Mouse naïve CD4⁺ lymphocytes were activated for four days with anti-CD3/CD28 antibodies under Th1-, Th17-, or Treg-cell-polarizing conditions. Cells were treated with indicated doses of DMF, MMF, or heptelidic acid on day 0 and assayed by flow cytometry on day 4. (A) DMF disproportionately decreased survival under Th1- and Th17-cell vs. Treg-cell polarizing conditions, as assessed by LIVE/DEAD aqua stain. Data represent mean ± SEM of three experiments performed in duplicate or triplicate. (B and C) DMF/MMF decreased the proportion of Tbet⁺ and IFNγ⁺ cells under Th1-cell-polarizing conditions (B) and of IL-17⁺ cells under Th17-cell-polarizing conditions (C, left). DMF (25 μM) produced variable results under Th17-cell-polarizing conditions, likely due to high toxicity at that dose, but nonetheless caused a significant decrease in total IL-17⁺ cell count (C, right). Data represent mean ± SEM of three experiments performed in duplicate or triplicate. (D) Representative flow cytometric plots demonstrating that low-dose (0.5 μM) heptelidic acid replicated the effect of DMF/MMF on IFNγ and IL-17 expression under Th1- and Th17-cell-polarizing conditions, respectively. Toxicity limited the testing of higher doses. Values represent mean ± SEM of a triplicate experiment. (E) In contrast to effects on Th1 and Th17 cells, DMF increased the proportion of FoxP3⁺ cells under Treg-cell-polarizing conditions. Data represent mean ± SEM of three experiments performed in duplicate or triplicate. (F) DMF/MMF produced a reciprocal increase in FoxP3⁺ cells under Th17-cell-polarizing conditions. Bar graph (left) and representative flow cytometric plot (right) from a triplicate experiment. Data represent mean ± SEM. (**G**) Mouse naïve CD4⁺ lymphocytes were activated under Th1- or Th17-cell-polarizing conditions for three days and then treated overnight with the indicated drug. Expression of IFNγ and IL-17 was then assessed by flow cytometry. Data represent mean ± SEM of a triplicate experiment. (**H**) Daily I.P. treatment with heptelidic acid attenuated the course of EAE. Data were pooled from five mice per group and represent mean ± SEM for each time point. (**I**) Proposed model of immune modulation by DMF, which may exploit a physiologic negative feedback function of endogenous fumarate. *$P < 0.05$ and **$P < 0.01$ by one-way ANOVA with Tukey's multiple comparison (A); one-way ANOVA with Dunnett's multiple comparison (B, C, E–G); and Mann–Whitney *U* test (H).

Dimethyl fumarate targets GAPDH and aerobic glycolysis to modulate immunity

Michael D. Kornberg, Pavan Bhargava, Paul M. Kim, Vasanta Putluri, Adele M. Snowman, Nagireddy Putluri, Peter A. Calabresi and Solomon H. Snyder

published online March 29, 2018